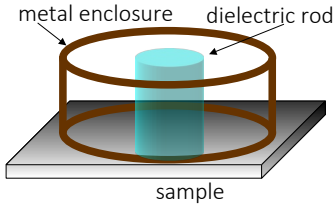


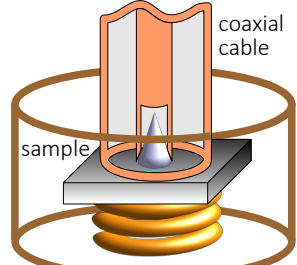
Microwave studies of the surface impedance of superconductors in the mixed state

Nicola
Pompeo

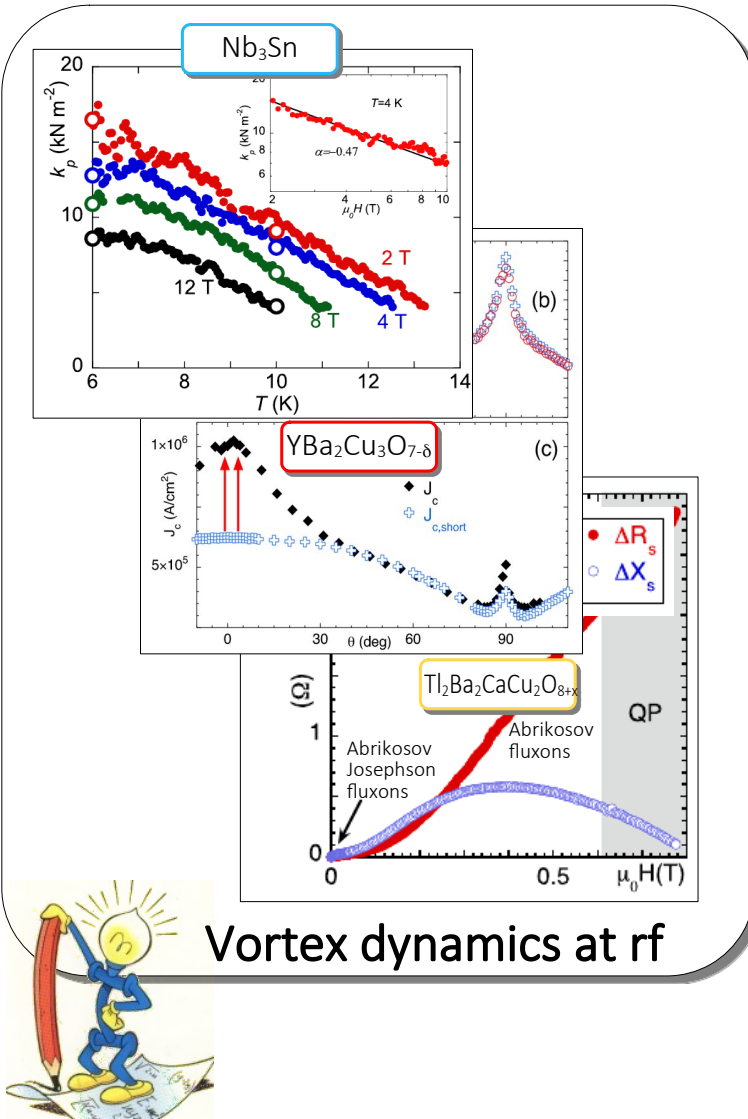
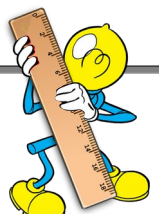
Measurement techniques



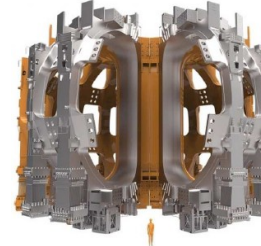
Dielectric-loaded Resonators
mono/dual frequency
8-48 GHz



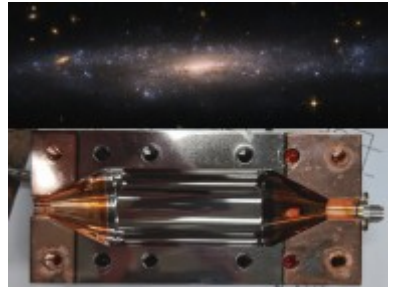
Corbino Disk
wide band
1-20 GHz



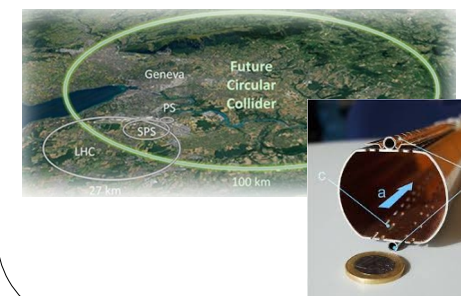
Input for applications



ITER
fusion reactor



Dark matter
search



Future Circular
Collider
Beam
screen

Electrodynamics of the Matter Lab

Nicola Pompeo*, Kostiantyn Torokhtii, Andrea Alimenti



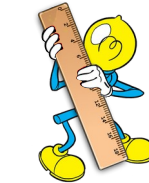
Group Leader
prof. E. Silva



*nicola.pompeo@uniroma3.it

Outline

- Measurand at microwaves: surface impedance Z_s
- High frequency vortex dynamics
- The techniques
 - dielectric resonators
 - Corbino disk
- Selected results:
 - Low T_c: Nb₃Sn, Nb
 - MgB₂
 - Cuprates: YBa₂Cu₃O_{7-δ}
 - Iron superconductors: FeSe_{0.5}Te_{0.5}
- Conclusions



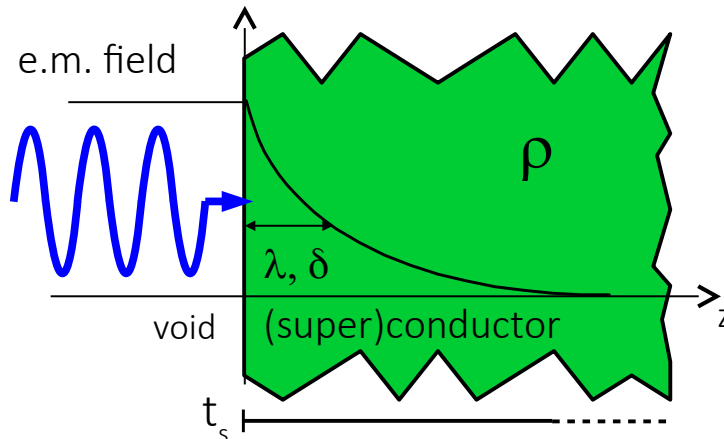
Surface impedance

Measurand at microwaves:

$$Z_s = \frac{E_{\parallel}}{H_{\parallel}} = R_s + iX_s$$

Bulk (super)conductor

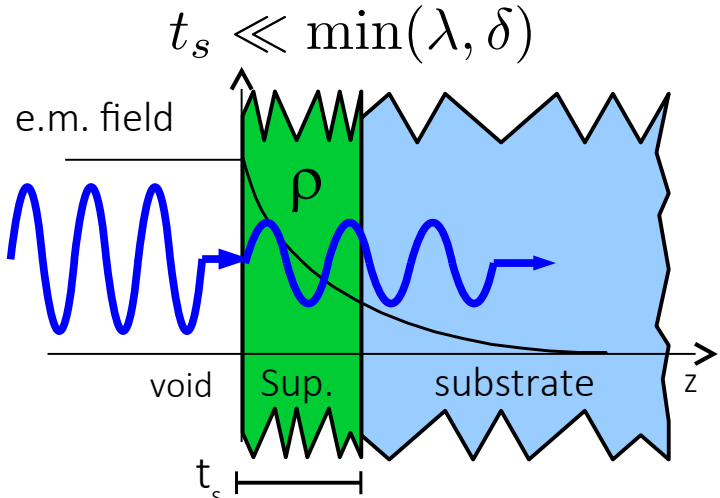
$$t_s \gg \max(\lambda, \delta)$$



$$Z_s = \sqrt{i2\pi\nu\mu_0\rho}$$

dissipation
reactive energy

Thin film on insulating substrate



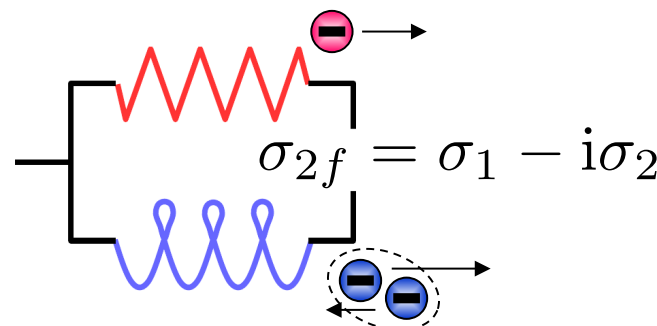
$$Z_s \approx \frac{\rho}{t_s}$$

Superconductor surface impedance

Zero field (Meissner state)

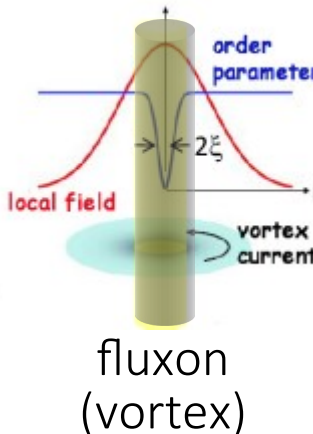
- Two fluid model

$$\sigma_1 = \frac{n_n e^2 \tau}{m}$$



$$\sigma_2 = \frac{n_s e^2}{m\omega} = \frac{\omega\mu_0}{\lambda^2}$$

In-field (Mixed state) (Type II SC)



- rf current $\Rightarrow F_L = J_{rf} \times \Phi_0$
 \Rightarrow oscillatory vortex motion
 \Rightarrow dissipation
- Material defects:
fluxon on defect lowers energy
 \Rightarrow pinning
 \Rightarrow dissipation reduction

vortex motion
resistivity ρ_{vm}

$$\rho = \frac{\rho_{vm} + i \frac{1}{\sigma_2}}{1 + i \frac{\sigma_1}{\sigma_2}}$$

Coffey, Clem PRB 67, 386 (1991)

no pair-breaking
($B \ll B_{c2}$)
 $\sigma_1/\sigma_2 \ll 1$ ($T < T_c$)

$$\Delta\rho(H) = \rho(H) - \rho(0) \simeq \rho_{vm}(H)$$

High frequency vortex motion response

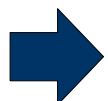
- $J_{rf} \rightarrow$ vortices oscillates around equilibrium positions (pins)
- Force balance (per unit length) (averaged over vortex length and vortices):
(vortex as massless damped harmonic oscillator)

$$\mathbf{J}_{rf} \times \Phi_0 - \eta \dot{\mathbf{u}} - k_p \mathbf{u} + \mathbf{F}_{thermal} = m \ddot{\mathbf{u}}$$

Driving force

$\mathbf{J}_{rf} \times \Phi_0$ Very short oscillations $< 1 \text{ nm}$

Viscous drag



Viscosity η

Flux flow resistivity ρ_{ff}

$$\rho_{ff} = \frac{\Phi_0 B}{\eta} = \alpha \rho_n \frac{B}{B_{c2}}$$

Pinning force



Pinning constant k_p

$$k_p = d^2 U / dx^2$$

$U(r)$: pinning energy profile

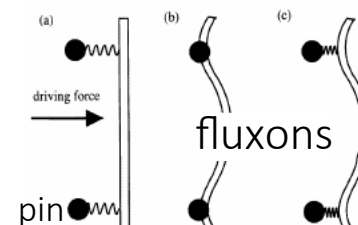
Stochastic thermal force

$\mathbf{F}_{thermal}$ Thermal activated jumps

Inertial term

$m \ddot{\mathbf{u}}$

Relevant at high (THz) frequency, neglected



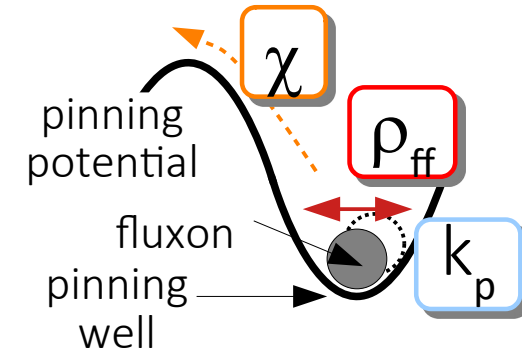
Vortex core physics

Vortex system physics

Gittleman, Rosenblum PRL 16 734 (1966)
Coffey, Clem PRL 67 386 (1991)
Brandt PRL 67 2219 (1991)
Golosovsky et al SUST 9 (1996)

High frequency vortex motion response

$$\mathbf{J}_{rf} \times \Phi_0 - \eta \dot{\mathbf{u}} - k_p \mathbf{u} + \mathbf{F}_{thermal} = m \ddot{\mathbf{u}} \rightarrow \mathbf{E} = \mathbf{B} \times \dot{\mathbf{u}} \Rightarrow \rho_{vm}$$

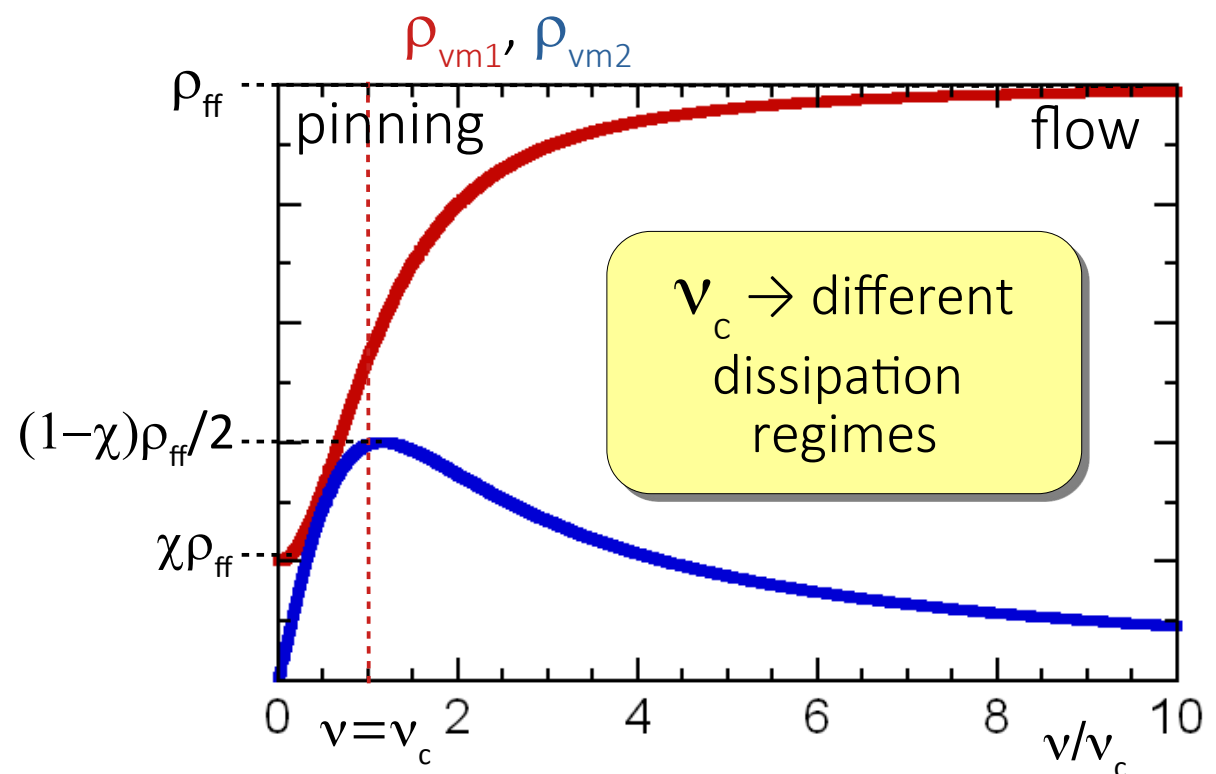


$$\rho_{vm} = \rho_{vm1} + i\rho_{vm2} = \rho_{ff} \frac{\chi + i\nu/\nu_c}{1 + i\nu/\nu_c}$$

Many models*,
one equation

Pompeo, Silva, PRB 78 , 094503 (2008)

*Gittleman, Rosenblum PRL 16 734 (1966) No creep
Coffey, Clem PRL 67 386 (1991) Sinusoidal potential
Brandt PRL 67 2219 (1991) Thermally relaxing pinning
Placais et al PRB 54 13083 (1996) Two-modes



characteristic freq. ν_c
pinning freq. ν_p

$\nu_c \xrightarrow{\chi \rightarrow 0} \nu_p$

related to pinning
barriers heights U_0
 $0 \leq \chi \leq 1$

creep factor χ

flux flow resistivity ρ_{ff}
viscosity η

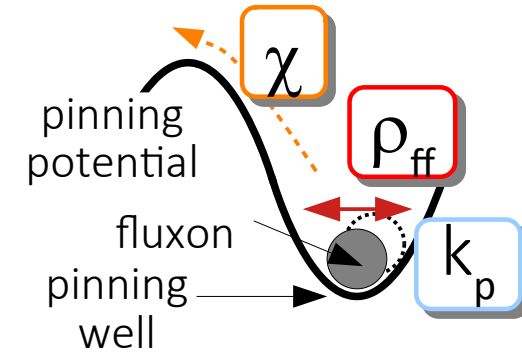
dissipation

pinning constant k_p

$k_p = 2\pi\nu_p\eta$

High frequency vortex motion response

$$\mathbf{J}_{rf} \times \Phi_0 - \eta \dot{\mathbf{u}} - k_p \mathbf{u} + \mathbf{F}_{thermal} = m \ddot{\mathbf{u}} \rightarrow \mathbf{E} = \mathbf{B} \times \dot{\mathbf{u}} \Rightarrow \rho_{vm}$$



$$\rho_{vm} = \rho_{vm1} + i\rho_{vm2} = \rho_{ff} \frac{\chi + i\nu/\nu_c}{1 + i\nu/\nu_c}$$

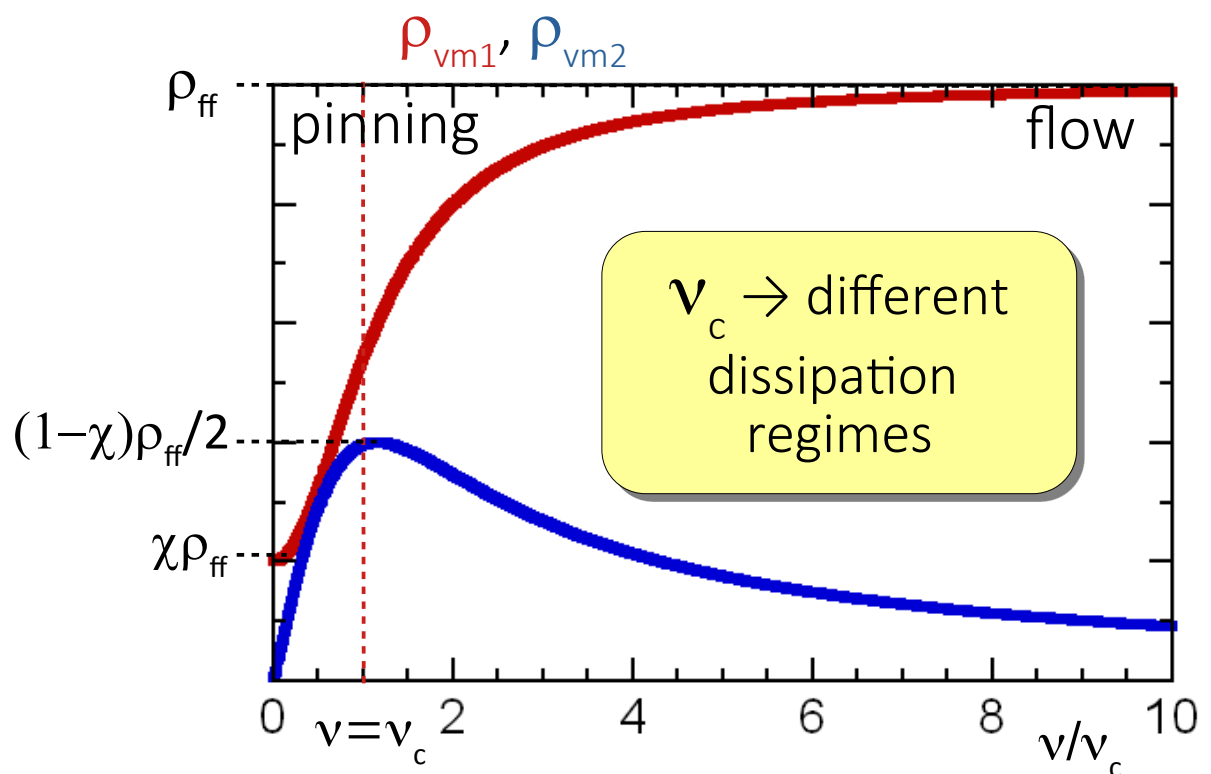
2 observables

3 parameters

Many models*,
one equation

Pompeo, Silva, PRB 78 , 094503 (2008)

*Gittleman, Rosenblum PRL 16 734 (1966) No creep
Coffey, Clem PRL 67 386 (1991) Sinusoidal potential
Brandt PRL 67 2219 (1991) Thermally relaxing pinning
Placais et al PRB 54 13083 (1996) Two-modes



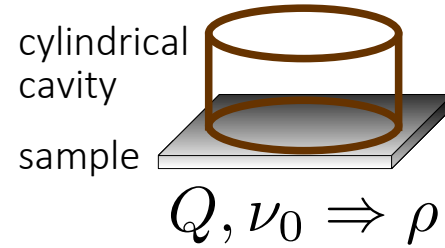
Multifrequency (rarely performed)

Outline

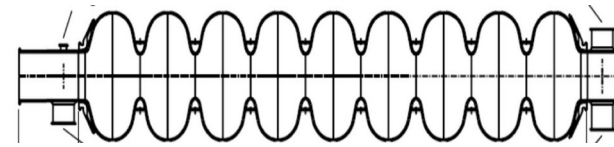
- Measurand at microwaves: surface impedance Z_s
- High frequency vortex dynamics
- The techniques
 - dielectric resonators
 - Corbino disk
- Selected results:
 - Low T_c: Nb₃Sn, Nb
 - MgB₂
 - Cuprates: YBa₂Cu₃O_{7-δ}
 - Iron superconductors: FeSe_{0.5}Te_{0.5}
- Conclusions



Cavity as a measurement instrument



VS

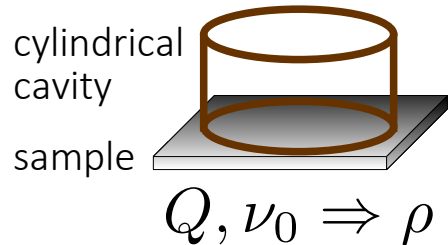


$$Q, \nu_0 \Rightarrow \vec{E}_{rf}$$

9-cell TESLA-type accelerating structure
H. Padamsee, Supercond. Sci. Technol. 30, 053003 (2017)

geometry for measurements of material properties?

Cavity as a measurement instrument



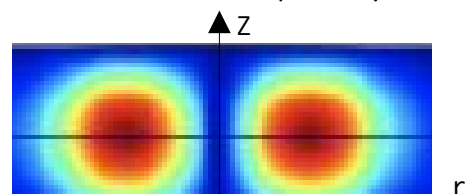
Resonant mode

$$Q = \frac{2\pi\nu_0 W}{P_{diss}}$$

quality factor

ν_0

resonant frequency



Spatial configuration
(TE, TM, TEM, HEM)

- sensitivity (Q^2/G) not optimal:
 - sample surface \ll whole surface
 - losses from metal enclosure

Perturbation theory

$$\frac{1}{Q} = \sum_i \frac{R_i}{G_i}$$

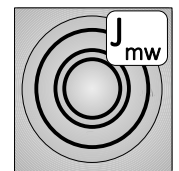
dissipation

$$\frac{\Delta\nu_0}{\nu_0} = \frac{W_H - W_E}{W} = - \sum_i \frac{\Delta X_i}{2G_i}$$

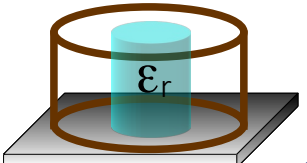
stored energy

W: stored energy
 P_{diss} : dissipated power
 G_i : geometrical factors
 (computed | calibrated)

- Cylindrical geometry (optimal Q)
- Mode: TE_{011}
 (probing currents: planar \rightarrow in-plane properties)



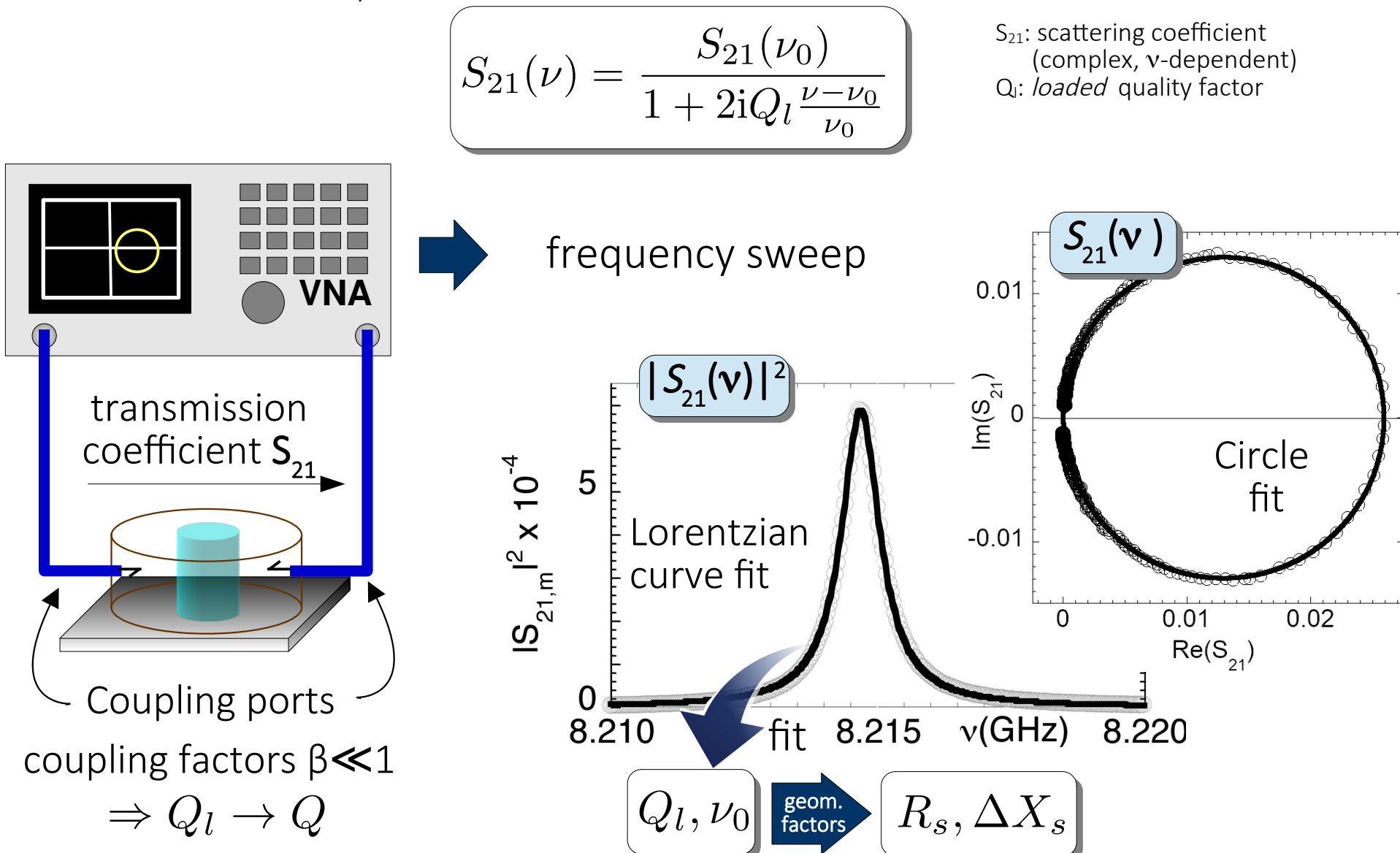
$\langle Z_s \rangle$ sample surface



- High sensitivity: dielectric loaded resonator
 - focus e.m. field \rightarrow reduces lateral losses
 - reduces overall size \rightarrow smaller samples
 - same enclosure for different rods/operating frequencies

Resonators: measurement of Q, ν_0 (basics)

- Operation in transmission, resonance curve:

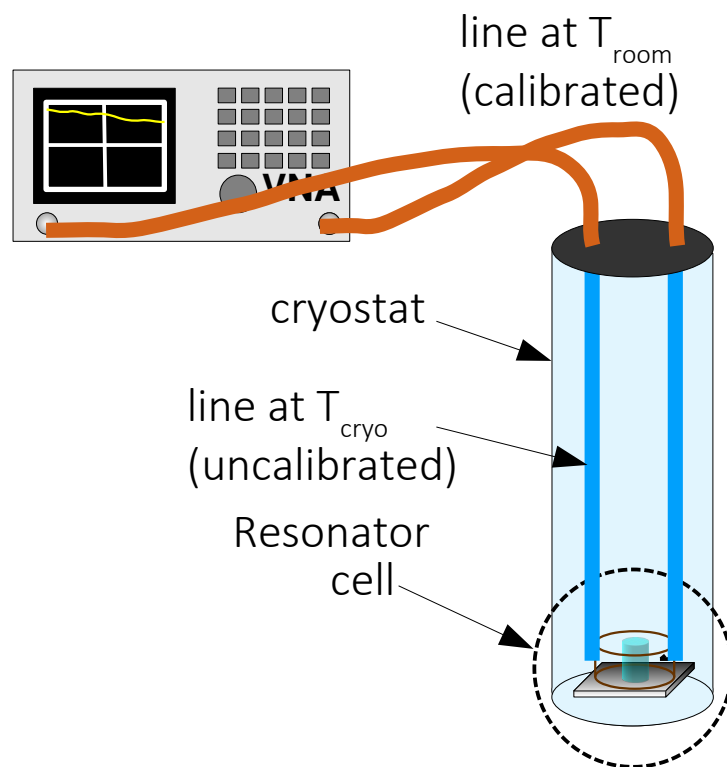
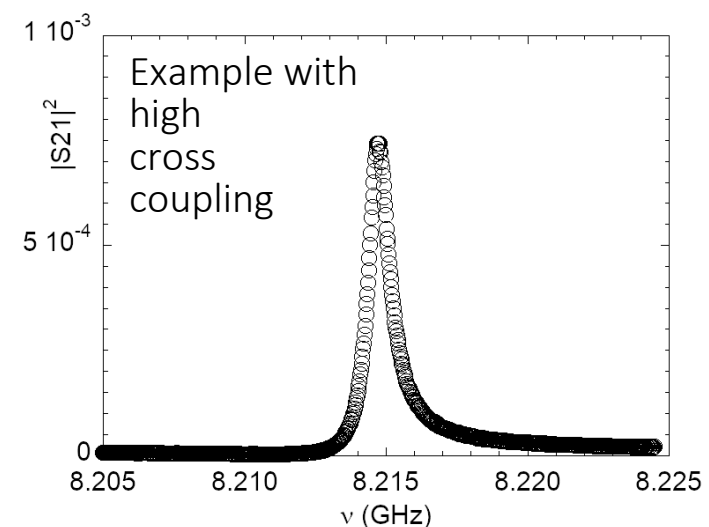


Resonators: measurement of Q, ν_0 (advanced)

- Non idealities on S_{21} → deformation of resonance curve
 - partially uncalibrated line
 - cross coupling between ports
 - interference from nearby modes



Extended models for S_{ij}



- Metrological aspects:
 - assessment of uncertainties in uncalibrated measurements
 - choice of optimal frequency span for minimum uncertainties on Q and ν_0

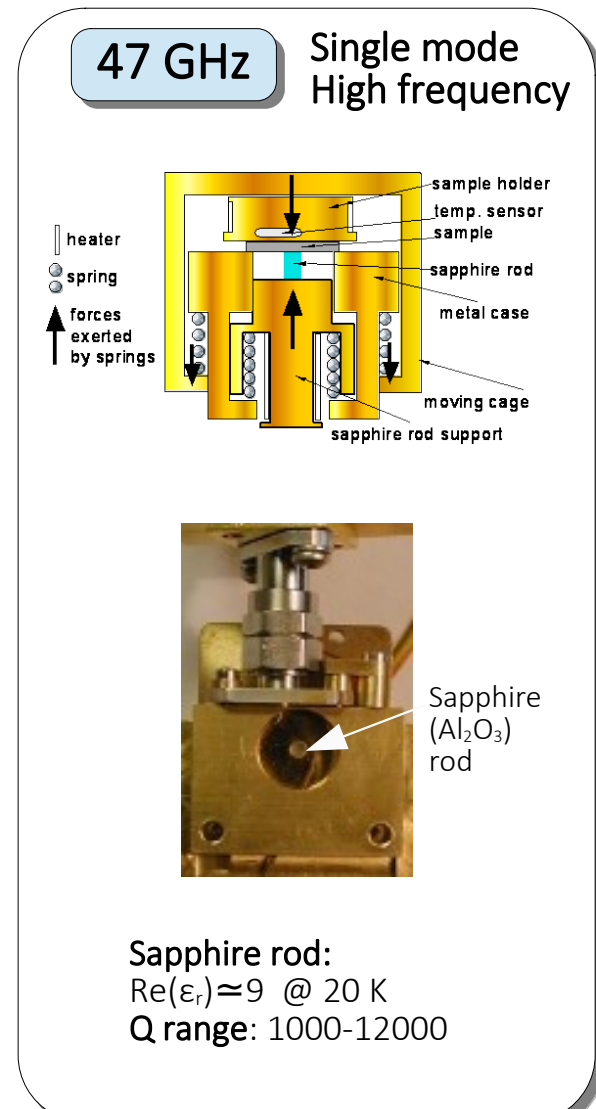
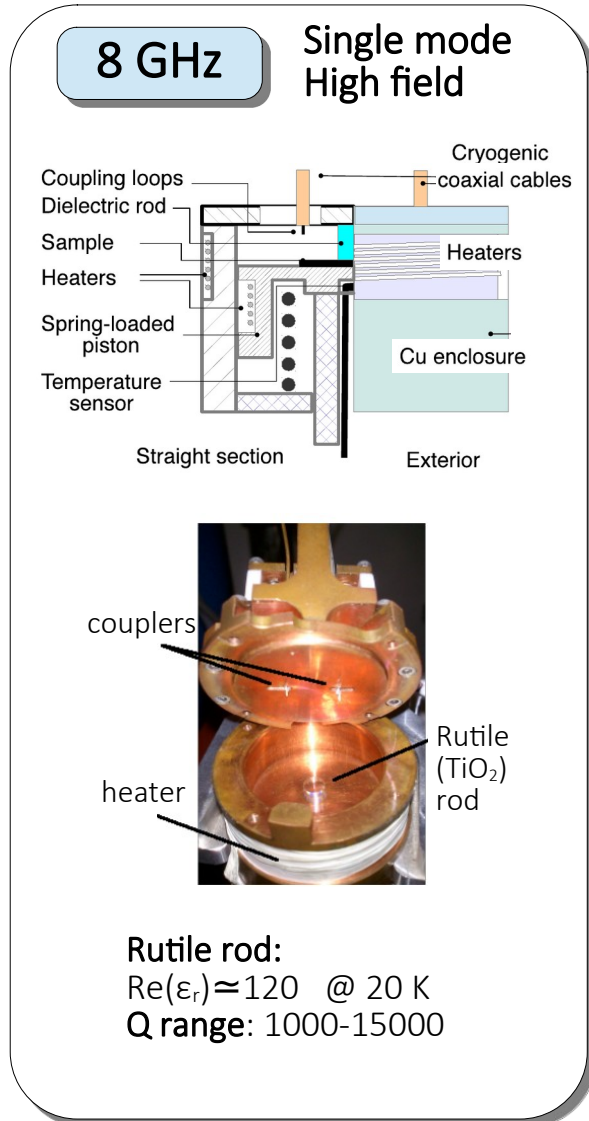
Torokhtii et al. "Frequency span optimization for asymmetric resonance curve fitting", Conf. Proc. I2MTC 2021
Alimenti et al. Meas. Sci. Technol. 30 065601 (2019)
Torokhtii et al. ActaMEKO 3 47 (2020)

Our dielectric resonators - some figures

General features:

- custom made
- compatible with cryostat space & cryogenic T
- compatible with fields 1-10 T

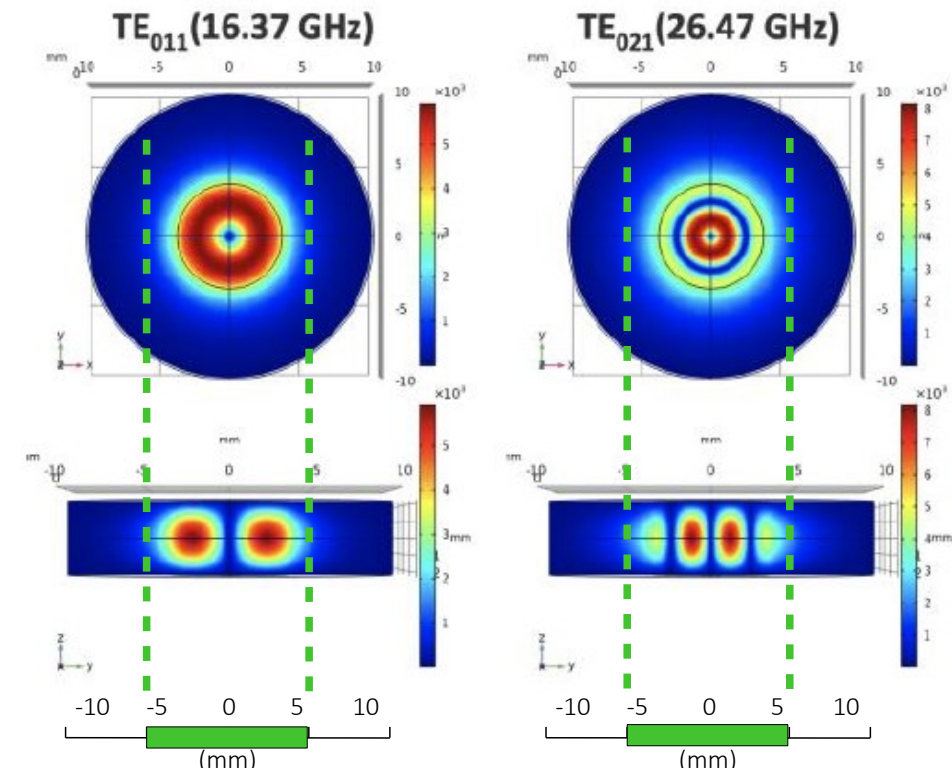
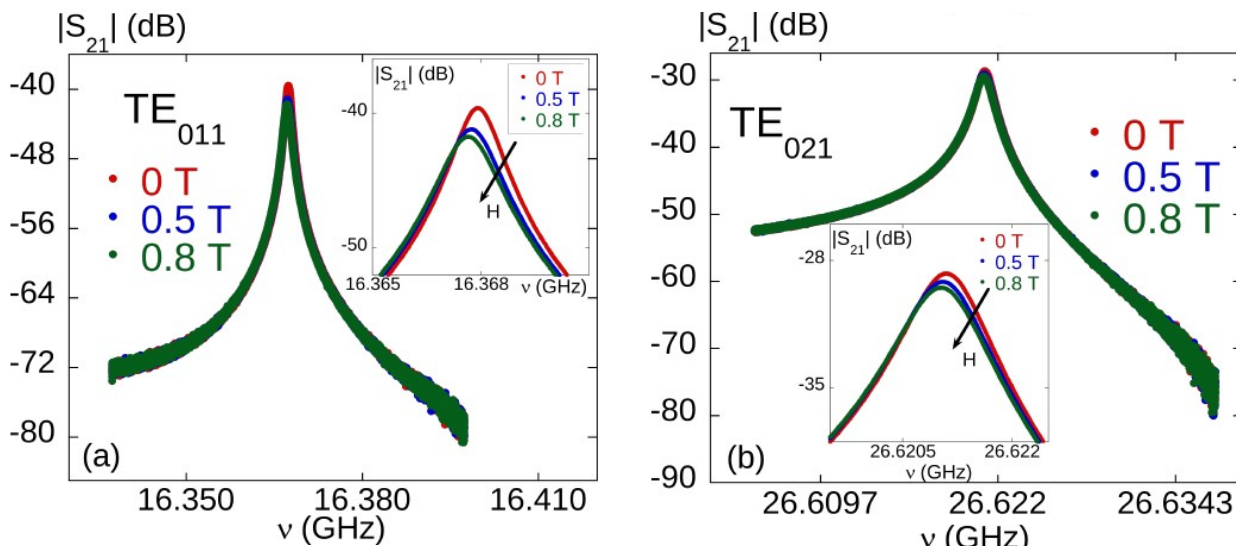
- Sample geometry: flat¶llel surfaces
- Probing area: $\varnothing \approx 3\text{-}10 \text{ mm}$



Multifrequency measurements

- Design criteria
 - well separated ν_0
 - well isolated modes
 - similar $J(r)$
- Modes: TE_{011} and TE_{021}

dual frequency operation
 $\nu_1=16.4$ GHz, $\nu_2=26.6$ GHz



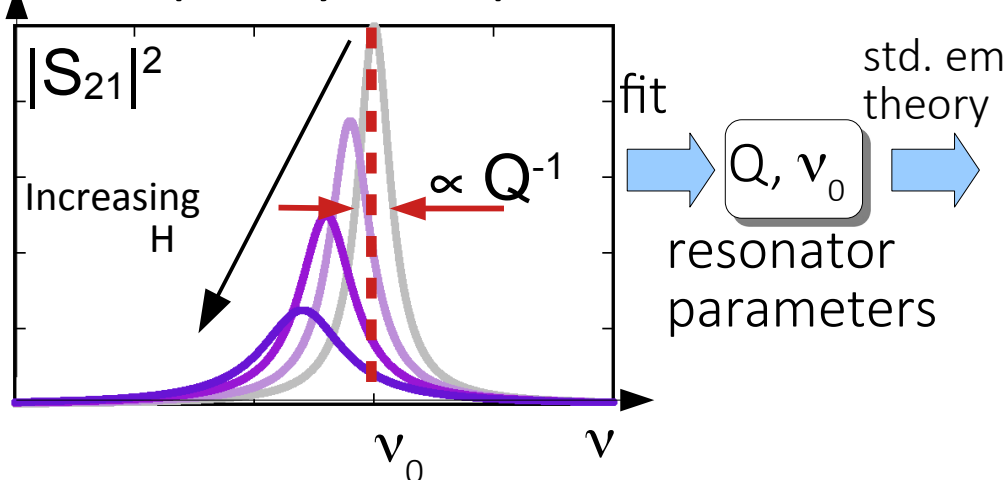
e.m. field profiles

Pompeo et al, 24th IMEKO TC4 Int. Symp. Proc. 2020
Pompeo et al, Measurement, submitted 2021

Resonator technique - the measurement process

Z_s vs H , fixed T

Frequency sweeps



H-induced variations:

$$\Delta R(H) = G \left(\frac{1}{Q(H)} - \frac{1}{Q(0)} \right)$$
$$\Delta X(H) = -2G \frac{\nu_0(H) - \nu_0(0)}{\nu_0(0)}$$

Z_s vs T , fixed H

- Z vs T : separate evaluation of resonator background

$$R_s(T, H) = \frac{G_s}{Q(T, H)} + \text{background}_R(T)$$

$$\Delta X_s(T, H) = -2G_s \frac{\Delta \nu_0(T, H)}{\nu_{0,ref}} + \text{background}_X(T)$$

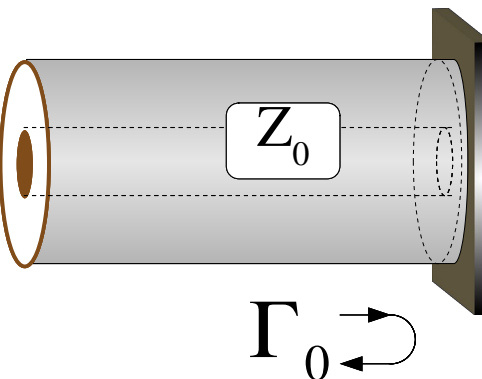
std. em theory

resonator parameters

$\rightarrow \Delta Z_s(H) \rightarrow \rho_{vm}$

Various limits:
- film/insulator $Z_s \propto \rho$
- bulk $Z_s \propto \sqrt{\rho}$
- film/metal (CC) $Z_s(\rho)$

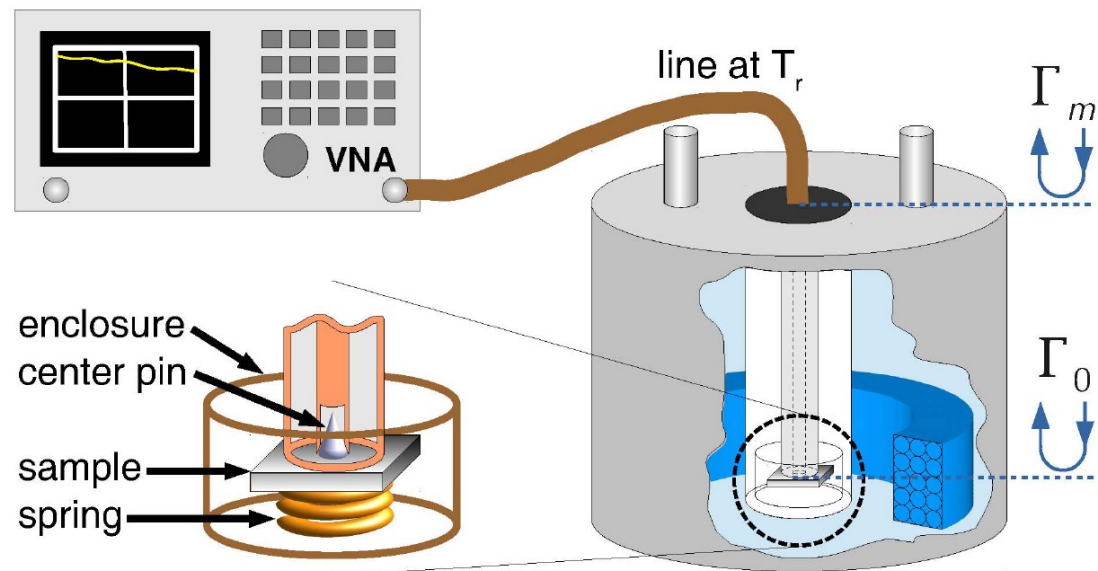
Corbino disk – microwave spectroscopy



$$Z_s(\nu) = Z_0 \frac{1 + \Gamma_0(\nu)}{1 - \Gamma_0(\nu)}$$

Γ_0 : (complex) reflection coefficient
 ν : frequency
 Z_0 : line characteristic impedance
 Z_s : sample impedance

- Main features
 - ✓ wide band (TEM mode): 1-25 GHz
 - ✓ mw currents J_{mw} :
 - planar → in-plane properties
 - subcritical → linear regime
- ✗ Approximate line calibration
 - various strategies

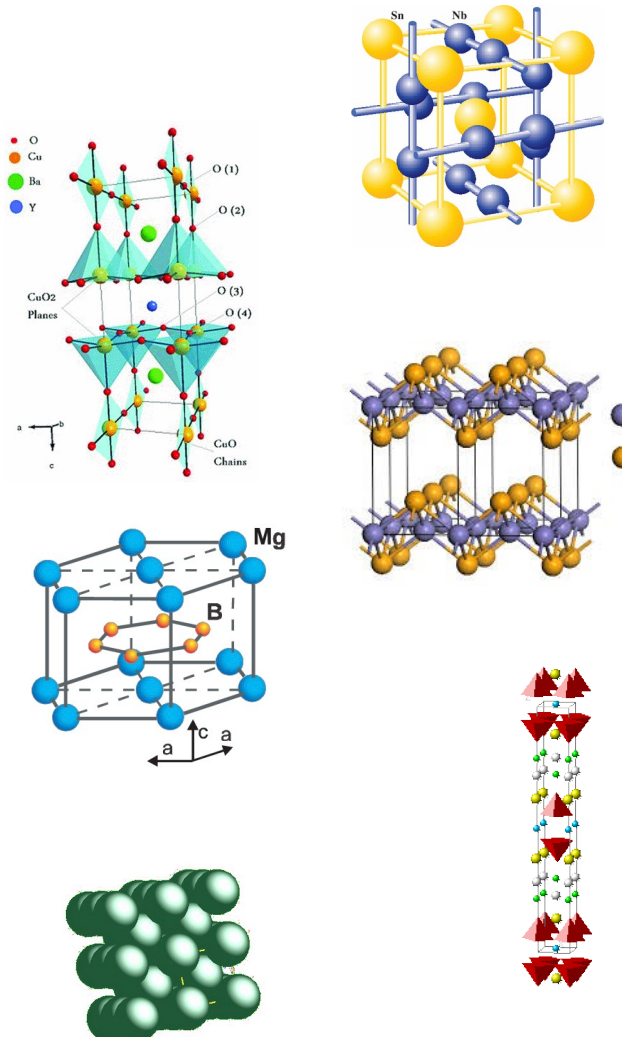


Outline

- Measurand at microwaves: surface impedance Z_s
- High frequency vortex dynamics
- The techniques
 - dielectric resonators
 - Corbino disk
- Selected results:
 - Low T_c: Nb₃Sn, Nb
 - MgB₂
 - Cuprates: YBa₂Cu₃O_{7-δ}
 - Iron superconductors: FeSe_{0.5}Te_{0.5}
- Conclusions



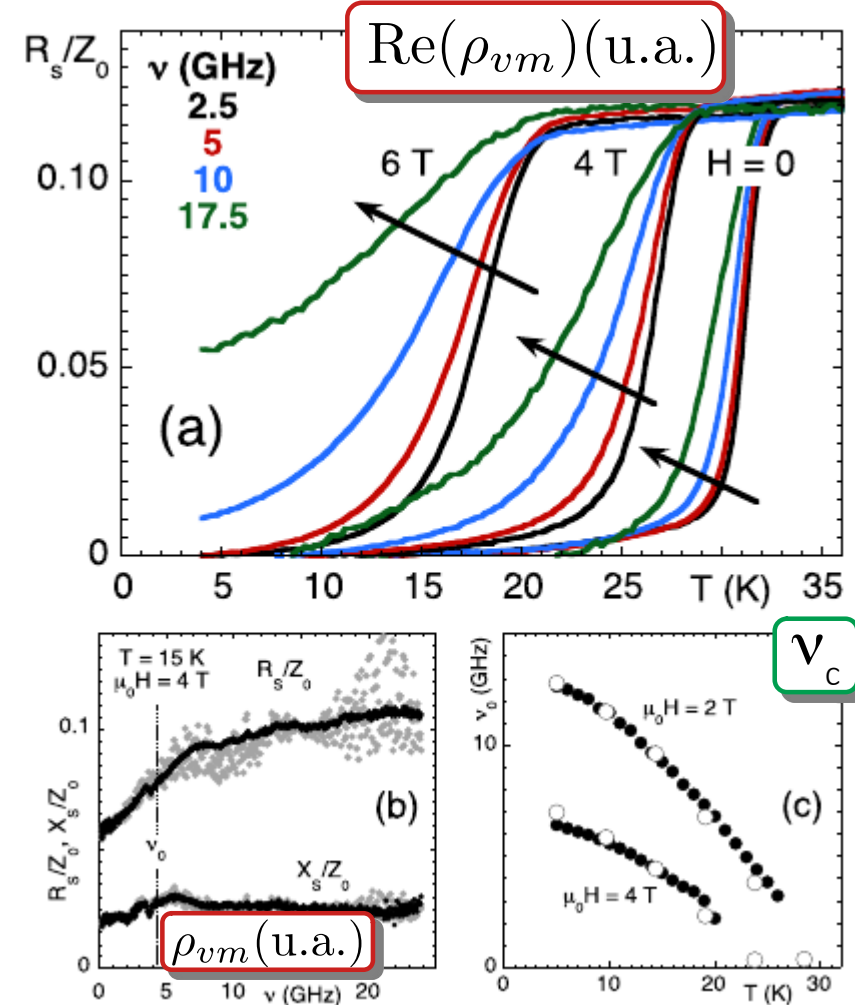
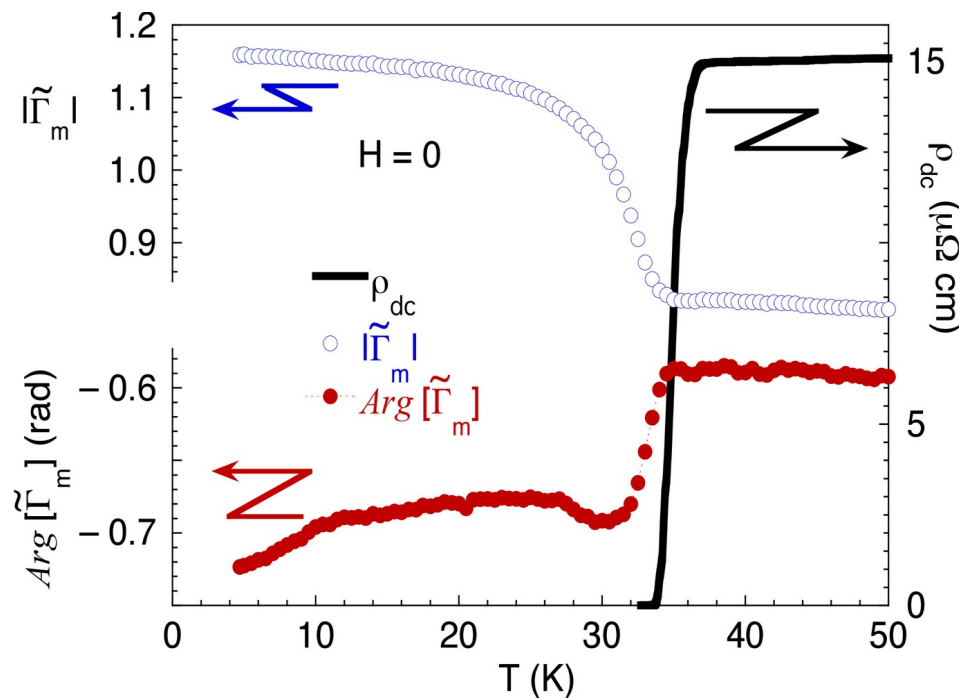
Studied materials



superconductor	T _c (K)	geometry	applications
Nb ₃ Sn	~18	bulk	haloscopes, RF cavities, cables
YBa ₂ Cu ₃ O _{7-δ}	~92	thin film coated conductor	beam screen coating (FCC), cables for fusion reactors, haloscopes
FeSe _{0.5} Te _{0.5}	~18	thin film	development of new coated conductor tapes
MgB ₂	~39	thin film bulk	PIT cables (CERN/fusion reactors), RF cavities
Tl ₂ Ba ₂ CaCu ₂ O _{8+x}	~110	thin film	
Nb	~9	thin film	RF cavities

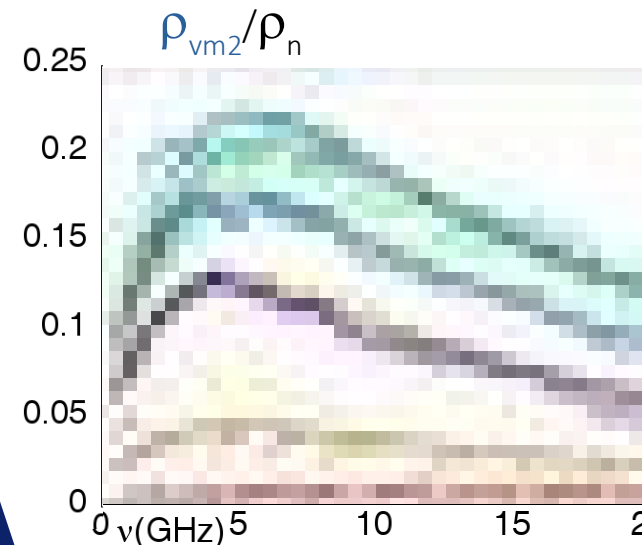
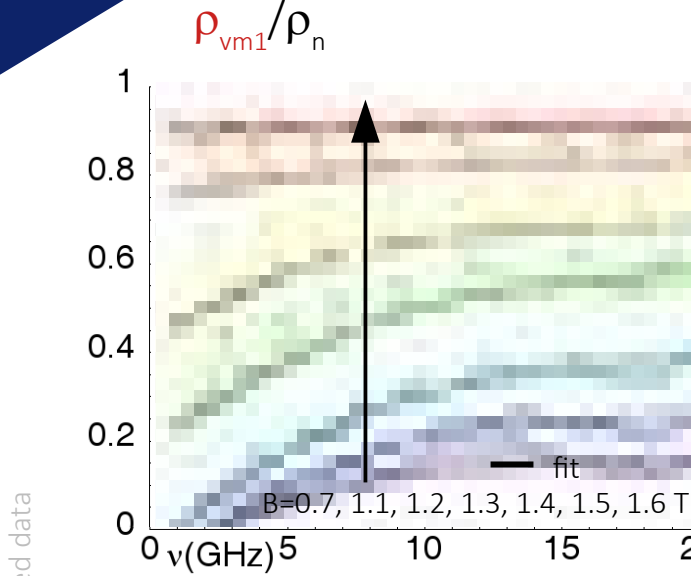
Corbino disk – example measurements (1)

MgB₂ thin film



Sarti et al, PRB 72 024542 (2005)
Silva et al, IEEE Trans. Instrum. Meas. 65 1120 (2016)

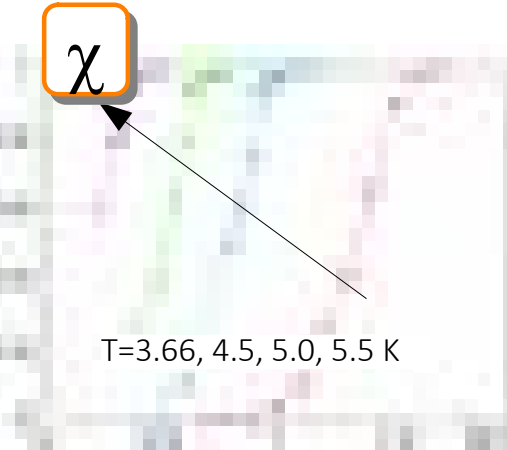
Corbino disk – example measurements (2)



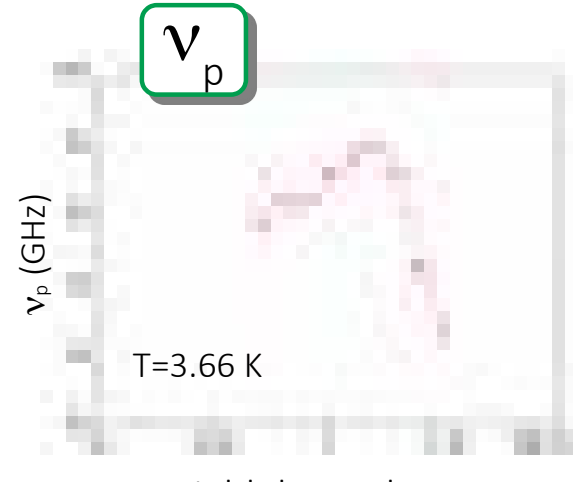
$t_s = 20 \text{ nm}$
 $\rho_n = 22 \text{ m}\Omega \text{ cm}$

Pompeo et al, Phys. C Supercond. 470 901 (2010)
Silva et al, SUST 24 024018 (2011)
Torokhtii et al, J. Supercond. 26 571 (2012)

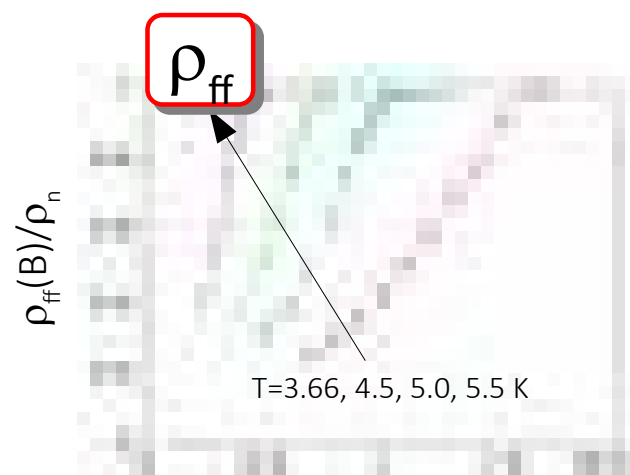
Nb thin film



Creep significantly $\neq 0$



Field dependent



deviation from simple
Bardeen-Stephen B-dep.

Nb₃Sn – High fields

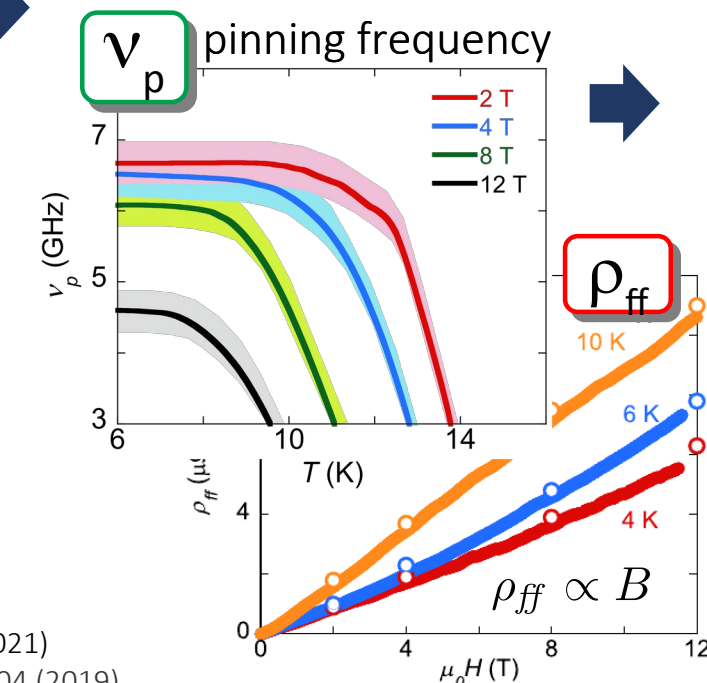
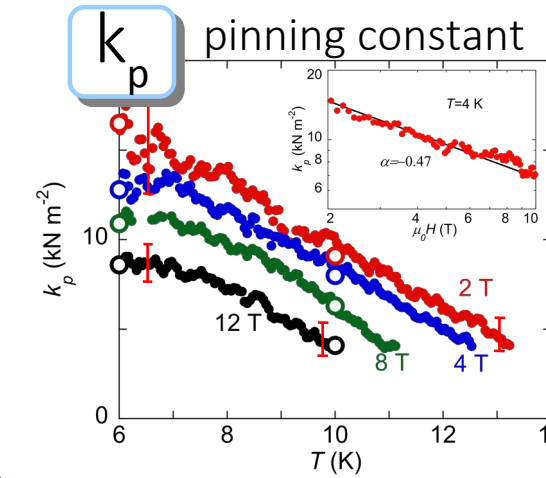
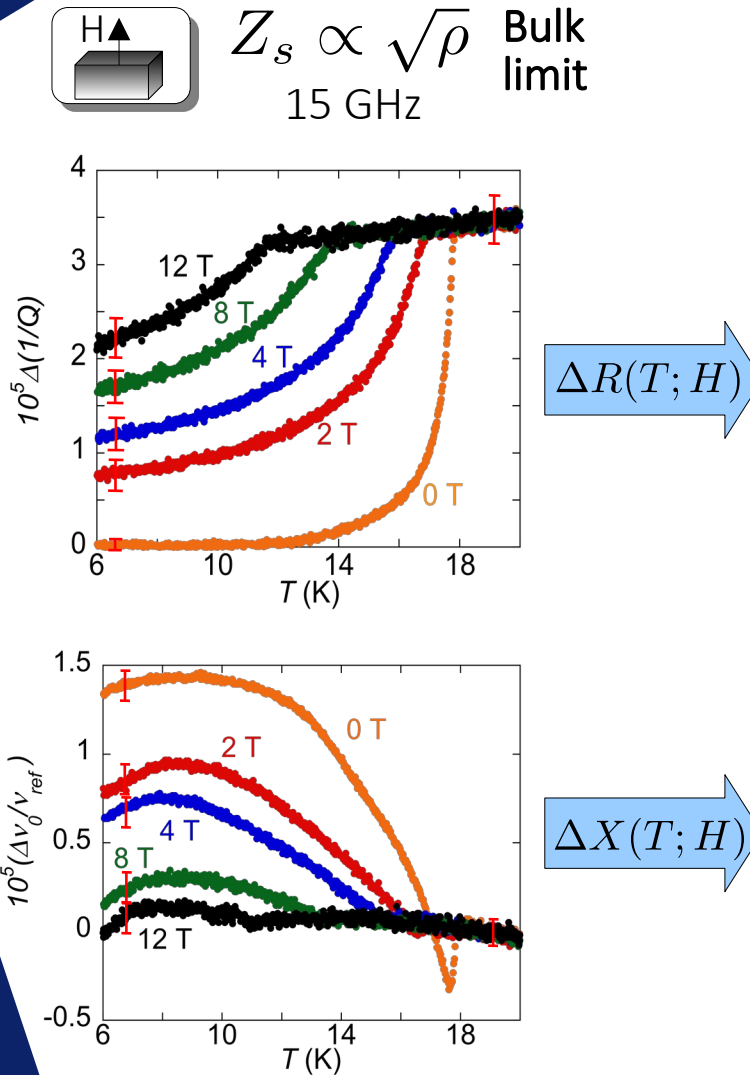
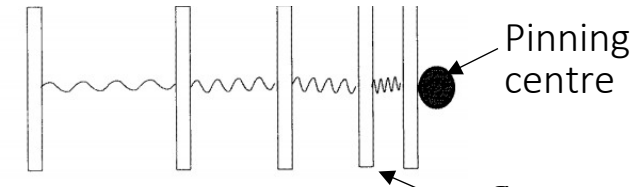
In collaboration with:

UNIVERSITÉ
DE GENÈVE

R. Flükiger

Fermilab

T. Spina

Field dependent \rightarrow Collective pinning regimeRoom for advanced material
engineering for rf improved pinning \sim operating frequencies of haloscopes but

Q @ (1 T, 9 GHz) of axion cavity

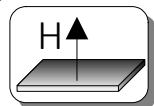
- Cu-based: 9×10^4 @ 4.2 K
- NbTi-based: 55×10^4 @ 4.2 K

Alesini et al PRD 99 101101 (2019)

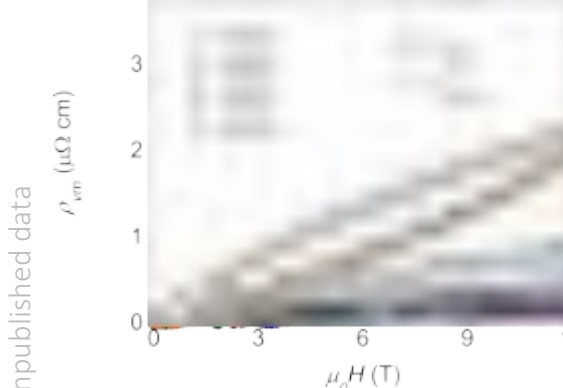
- Nb₃Sn-based: $< 7.5 \times 10^4$ @ 4.2 K (computed)

consistent with Bardeen-Stephen model
material "intrinsic" property

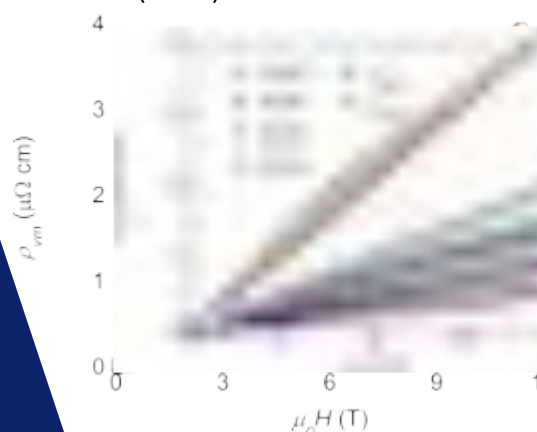
$\text{YBa}_2\text{Cu}_3\text{O}_{7-\delta}$ – High fields

 $Z_s = \rho/t_s$ thin film
15 GHz

Pulsed Laser Deposition (PLD)
pristine YBCO



Chemical Solution Deposition (CSD) – YBCO + 5% BaZrO₃



Alimenti et al - paper in preparation

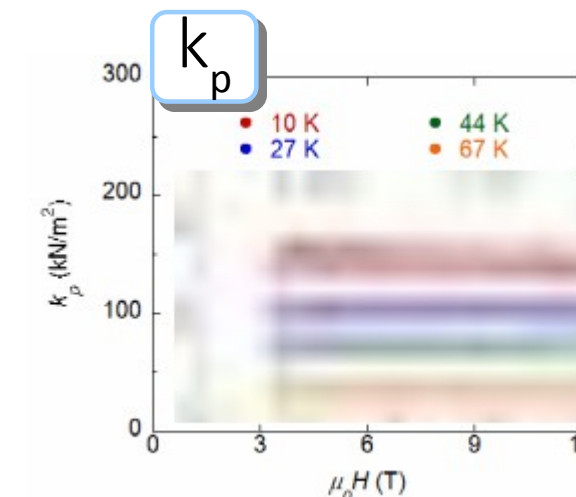
Supported by:
 EUROfusion

In collaboration with:
 ENEA
Agenzia nazionale per le nuove tecnologie,
l'energia e lo sviluppo economico sostenibile

 ICMAB
INSTITUT DE CIÈNCIA DE MATERIALS DE BARCELONA

G. Celentano

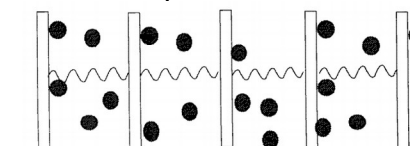
A. Palau



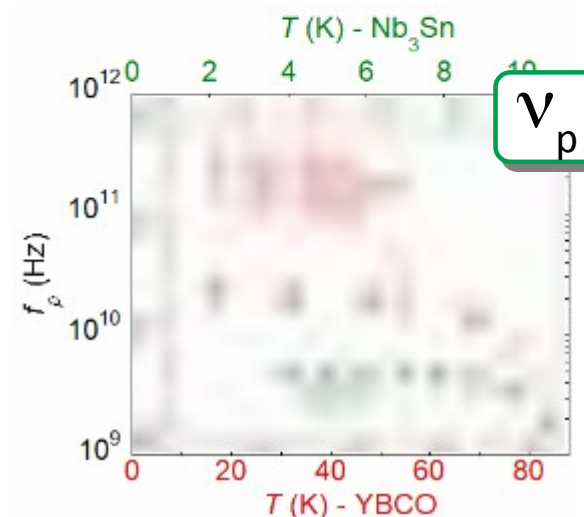
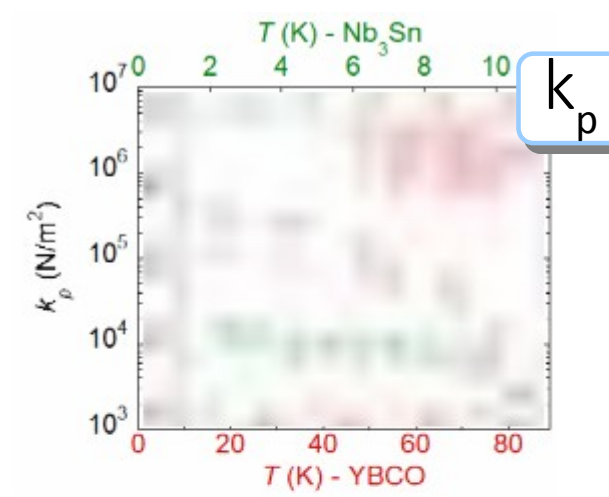
Field independent



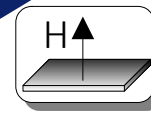
Fluxons individually pinned



- Best rf performances for the PLD-YBCO
- Higher than Nb₃Sn
- Particularly suitable for rf applications – FCC

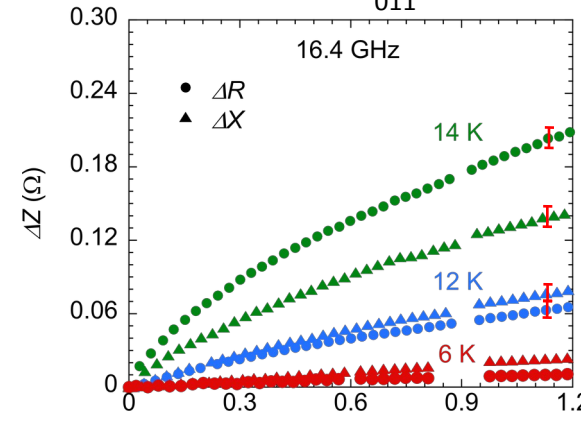


FeSe_{0.5}Te_{0.5} – multifreq.

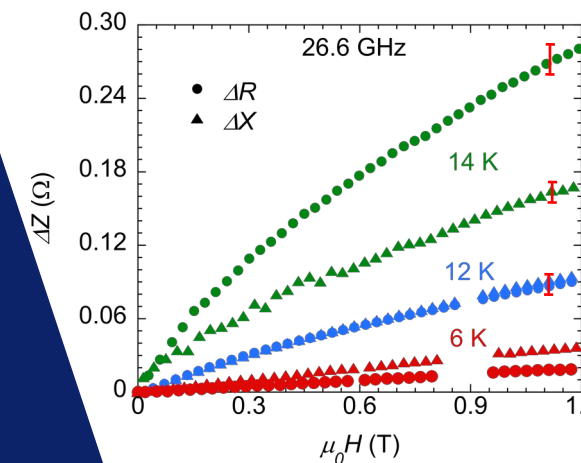


$$Z_s = \rho/t_s \text{ thin film}$$

TE₀₁₁ $t_s = 240$ nm

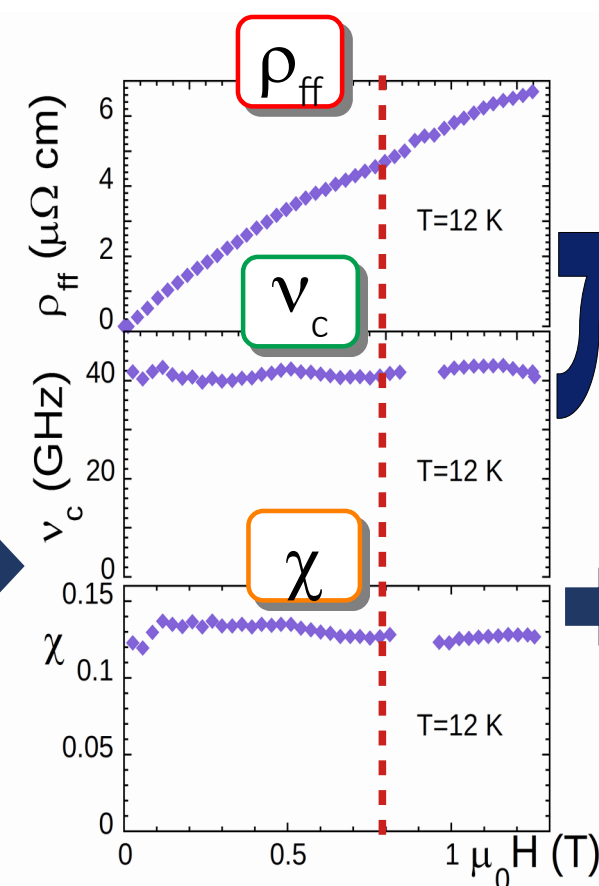


TE₀₂₁



Pompeo et al SuST 33 114006 (2020)

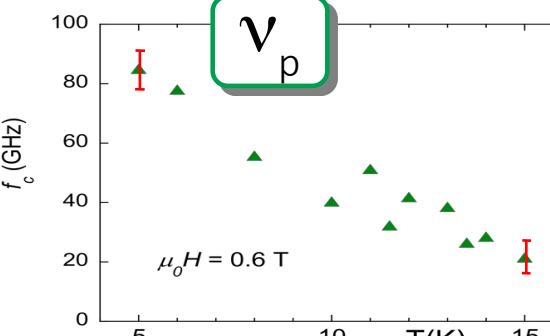
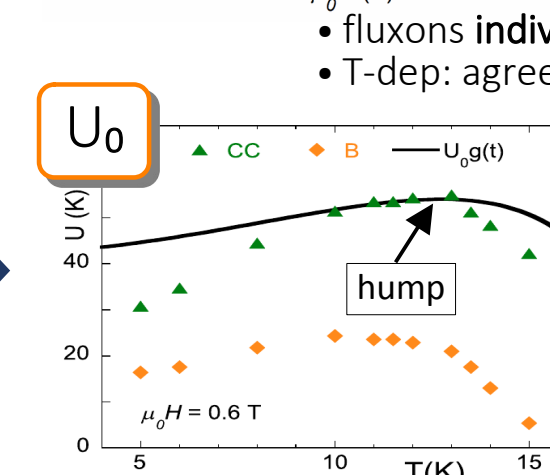
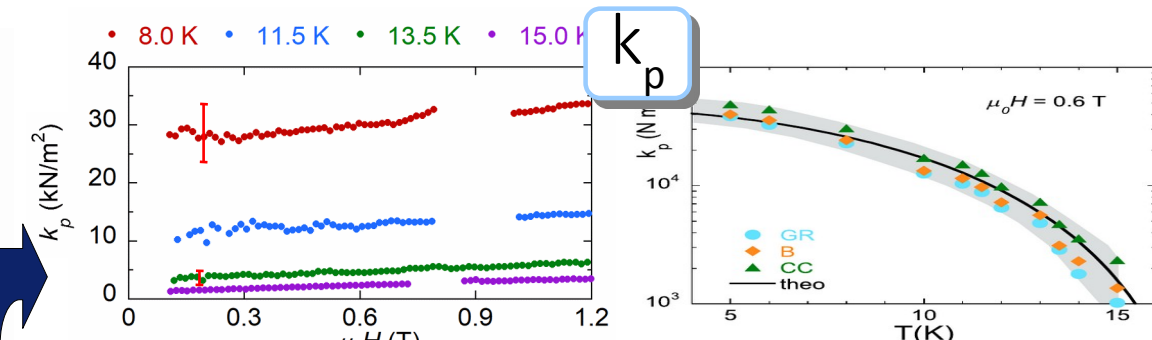
Pompeo et al IEEE Trans. Appl. Supercond. doi:10.1109/TASC.2021.3063665 (2021)



Supported by:
PRIN
HIBISCUS

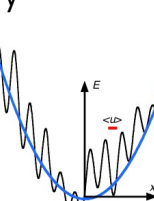


UNIVERSITÀ DEGLI STUDI
DI GENOVA
M. Putti



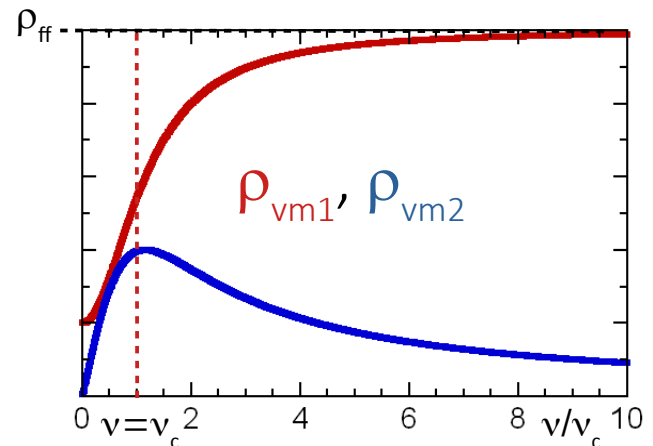
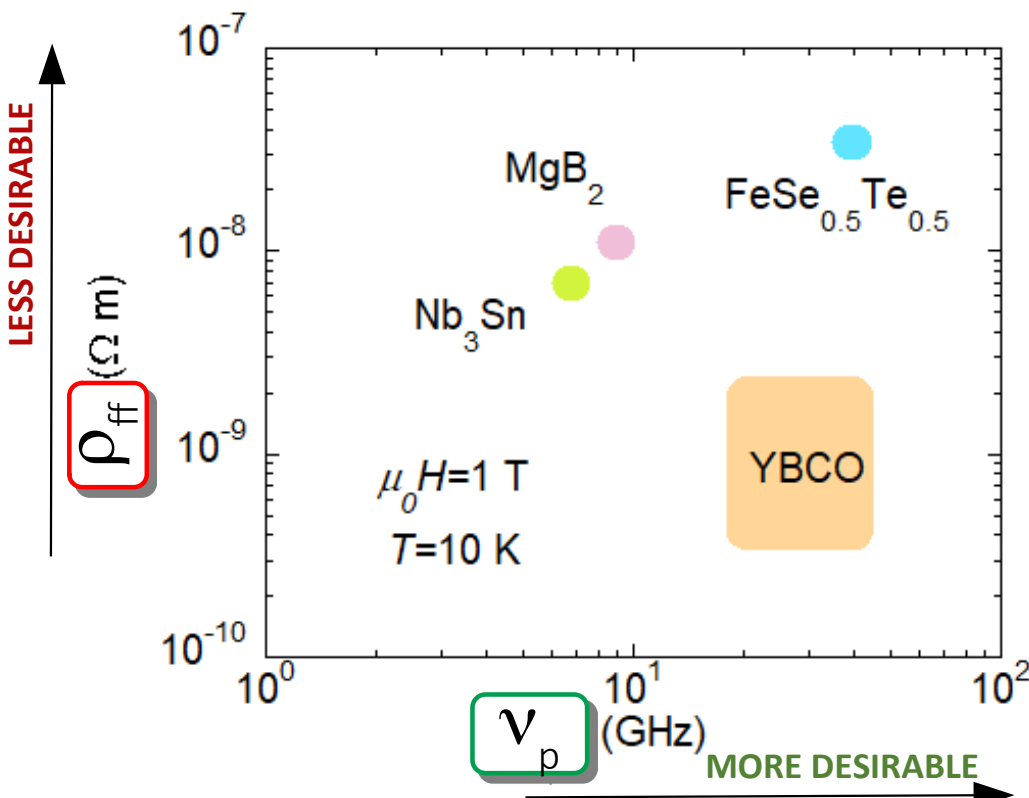
- fluxons individually pinned
- T-dep: agreement with theory

- ξ^3 volumes jumping by thermal activation “point” pins
- U_0 much smaller wrt other techniques



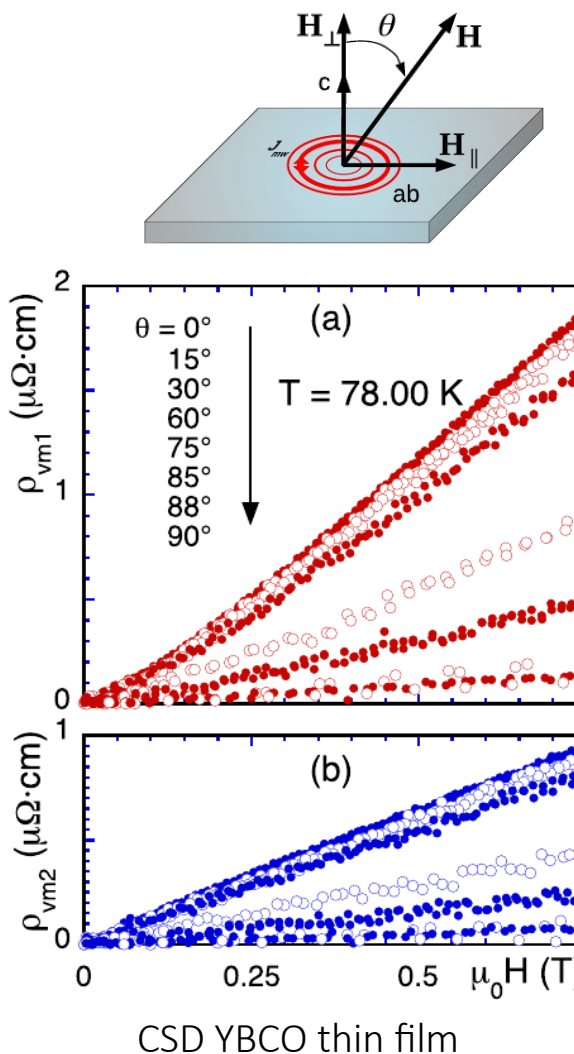
- $v_p(\text{FeSeTe}) > v_p(\text{YBCO}) \Rightarrow$ lower losses?

rf vortex motion - physical comparison

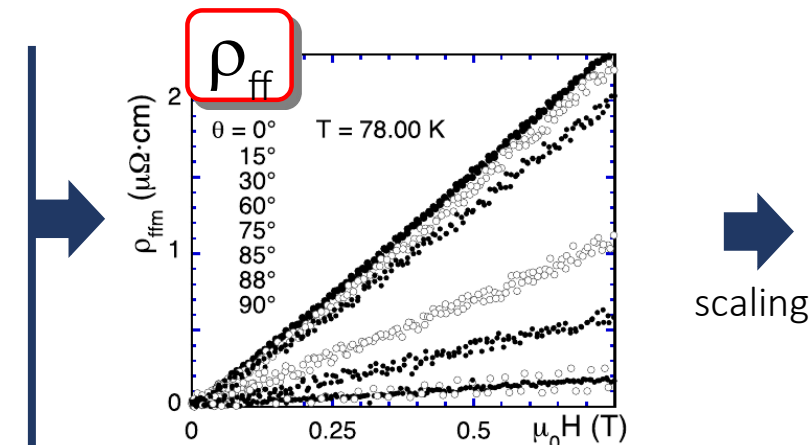


- YBCO: high v_p , lowest ρ_{ff}
- high $v_p \not\Rightarrow$ lowest losses

Angle dependent measurements – mass anisotropy



Pompeo et al SuST 33 044017 (2020)
 Bartolomé et al SuST 33 74006 (2020)
 Bartolomé et al PRB 100 054502 (2019)

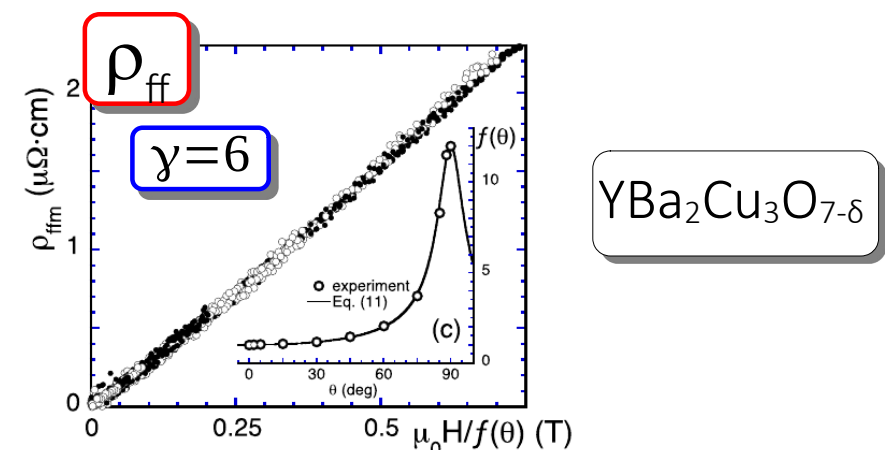


BGL scaling
 Blatter, Geshkenbein and Larkin PRL 68 875 (1992)

$$\begin{aligned} \mathcal{Q}(H, \theta) &= s_{\mathcal{Q}}(\theta) \mathcal{Q}(H \epsilon(\theta)) \\ \epsilon(\theta) &= (\gamma^{-2} \sin^2 \theta + \cos^2 \theta)^{1/2} \end{aligned}$$

Scaling of measured ρ_{ff}
 $\rho_{ff}(H, \theta)$ vs $H/f(\theta)$
 $f(\theta) = \epsilon(\theta)^{-1} f_L(\theta)^{1/\beta}$
 $f_L(\theta) = \frac{\gamma^{-2} \sin(\theta)^2 + \cos(\theta)^2}{\frac{\gamma^{-2}}{2} \sin(\theta)^2 + \cos(\theta)^2}$
 angle dependent Lorentz term

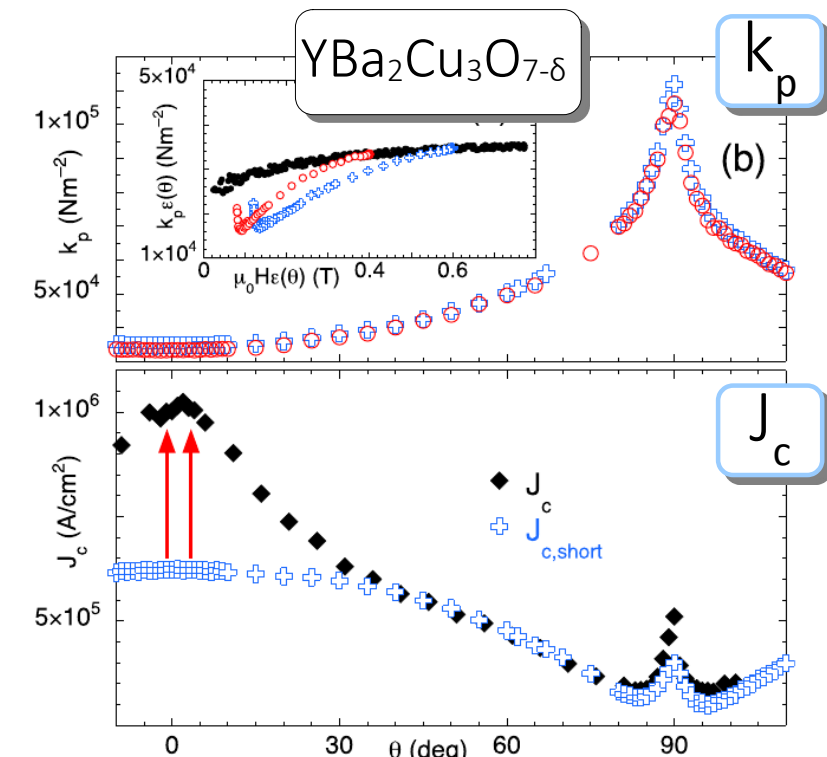
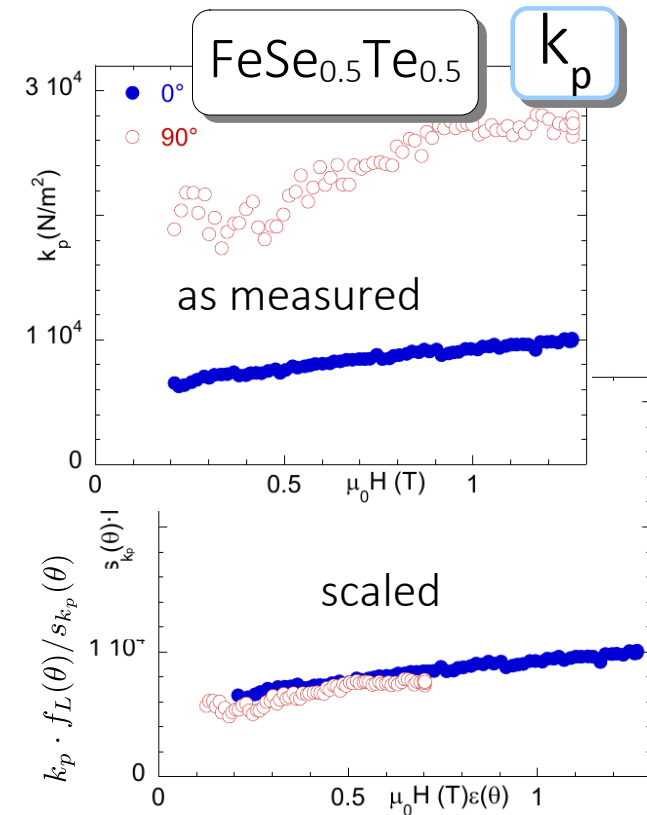
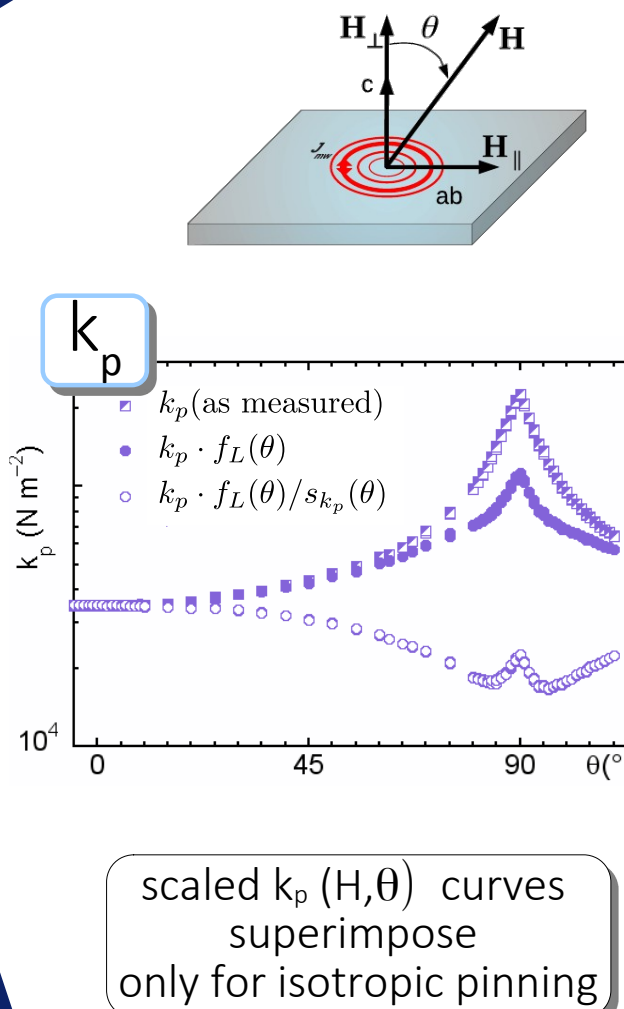
γ mass anisotropy (intrinsic)



Pompeo et al IEEE Trans. Appl. Supercond. doi:10.1109/TASC.2021.3063665 (2021)

Nicola Pompeo – 18-03-2021 – Jefferson Lab

Angle dependent measurements – pinning anisotropy



- 1) $k_p(H, \theta)$ curves do not superimpose
→ **anisotropic (correlated) pinning**
- 2) $J_c(\theta)$ vs $J_{c,short}(H, \theta) = c \frac{k_p(H, \theta) \xi_{ab} \epsilon(\theta)}{\Phi_0}$
(d.c. vs rf regimes):
different time-scales
→ different **dynamical effects**

Conclusions

- Surface impedance measurement techniques
 - Multifrequency dielectric resonator: sensitive, measurements vs frequency
 - Corbino disk: wide band, for niche studies
- High frequency vortex dynamics
 - many physical aspects (vortex core/system physics, pinning, anisotropy)
 - relevance of multifrequency measurements for
 - correct determination of all the relevant vortex parameters (ρ_{ff} , v_c , creep)
 - accurate extrapolation of Z_s at different (lower) frequencies
- The materials
 - Low T_c: Nb₃Sn – improvements on pinning needed
 - Cuprates: YBa₂Cu₃O_{7-δ} – best performances, candidate for FCC beam screen
 - Iron sc: FeSe_{0.5}Te_{0.5} – high pinning frequency but significant dissipation

Thanks for the attention